

Measurement of the B_c^+ Meson Lifetime Using the Decay Mode $B_c^+ \rightarrow J/\psi e^+ \nu_e$

- A. Abulencia,²³ D. Acosta,¹⁷ J. Adelman,¹³ T. Affolder,¹⁰ T. Akimoto,⁵⁵ M. G. Albrow,¹⁶ D. Ambrose,¹⁶ S. Amerio,⁴³ D. Amidei,³⁴ A. Anastassov,⁵² K. Anikeev,¹⁶ A. Annovi,¹⁸ J. Antos,¹ M. Aoki,⁵⁵ G. Apollinari,¹⁶ J.-F. Arguin,³³ T. Arisawa,⁵⁷ A. Artikov,¹⁴ W. Ashmanskas,¹⁶ A. Attal,⁸ F. Azfar,⁴² P. Azzi-Bacchetta,⁴³ P. Azzurri,⁴⁶ N. Bacchetta,⁴³ H. Bachacou,²⁸ W. Badgett,¹⁶ A. Barbaro-Galtieri,²⁸ V. E. Barnes,⁴⁸ B. A. Barnett,²⁴ S. Baroiant,⁷ V. Bartsch,³⁰ G. Bauer,³² F. Bedeschi,⁴⁶ S. Behari,²⁴ S. Belforte,⁵⁴ G. Bellettini,⁴⁶ J. Bellinger,⁵⁹ A. Belloni,³² E. Ben Haim,⁴⁴ D. Benjamin,¹⁵ A. Beretvas,¹⁶ J. Beringer,²⁸ T. Berry,²⁹ A. Bhatti,⁵⁰ M. Binkley,¹⁶ D. Bisello,⁴³ R. E. Blair,² C. Blocker,⁶ B. Blumenfeld,²⁴ A. Bocci,¹⁵ A. Bodek,⁴⁹ V. Boisvert,⁴⁹ G. Bolla,⁴⁸ A. Bolshov,³² D. Bortoletto,⁴⁸ J. Boudreau,⁴⁷ A. Boveia,¹⁰ B. Brau,¹⁰ C. Bromberg,³⁵ E. Brubaker,¹³ J. Budagov,¹⁴ H. S. Budd,⁴⁹ S. Budd,²³ K. Burkett,¹⁶ G. Busetto,⁴³ P. Bussey,²⁰ K. L. Byrum,² S. Cabrera,¹⁵ M. Campanelli,¹⁹ M. Campbell,³⁴ F. Canelli,⁸ A. Canepa,⁴⁸ D. Carlsmith,⁵⁹ R. Carosi,⁴⁶ S. Carron,¹⁵ M. Casarsa,⁵⁴ A. Castro,⁵ P. Catastini,⁴⁶ D. Cauz,⁵⁴ M. Cavalli-Sforza,³ A. Cerri,²⁸ L. Cerrito,⁴² S. H. Chang,²⁷ J. Chapman,³⁴ Y. C. Chen,¹ M. Chertok,⁷ G. Chiarelli,⁴⁶ G. Chlachidze,¹⁴ F. Chlebana,¹⁶ I. Cho,²⁷ K. Cho,²⁷ D. Chokheli,¹⁴ J. P. Chou,²¹ P. H. Chu,²³ S. H. Chuang,⁵⁹ K. Chung,¹² W. H. Chung,⁵⁹ Y. S. Chung,⁴⁹ M. Ciljak,⁴⁶ C. I. Ciobanu,²³ M. A. Ciocci,⁴⁶ A. Clark,¹⁹ D. Clark,⁶ M. Coca,¹⁵ G. Compostella,⁴³ M. E. Convery,⁵⁰ J. Conway,⁷ B. Cooper,³⁰ K. Copic,³⁴ M. Cordelli,¹⁸ G. Cortiana,⁴³ F. Crescioli,⁴⁶ A. Cruz,¹⁷ C. Cuenca Almenar,⁷ J. Cuevas,¹¹ R. Culbertson,¹⁶ D. Cyr,⁵⁹ S. DaRonco,⁴³ S. D'Auria,²⁰ M. D'Onofrio,³ D. Dagenhart,⁶ P. de Barbaro,⁴⁹ S. De Cecco,⁵¹ A. Deisher,²⁸ G. De Lentdecker,⁴⁹ M. Dell'Orso,⁴⁶ F. Delli Paoli,⁴³ S. Demers,⁴⁹ L. Demortier,⁵⁰ J. Deng,¹⁵ M. Deninno,⁵ D. De Pedis,⁵¹ P. F. Derwent,¹⁶ T. Devlin,⁵² C. Dionisi,⁵¹ J. R. Dittmann,⁴ P. DiTuro,⁵² C. Dörr,²⁵ S. Donati,⁴⁶ M. Donega,¹⁹ P. Dong,⁸ J. Donini,⁴³ T. Dorigo,⁴³ S. Dube,⁵² K. Ebina,⁵⁷ J. Efron,³⁹ J. Ehlers,¹⁹ R. Erbacher,⁷ D. Errede,²³ S. Errede,²³ R. Eusebi,¹⁶ H. C. Fang,²⁸ S. Farrington,²⁹ I. Fedorko,⁴⁶ W. T. Fedorko,¹³ R. G. Feild,⁶⁰ M. Feindt,²⁵ J. P. Fernandez,³¹ R. Field,¹⁷ G. Flanagan,⁴⁸ L. R. Flores-Castillo,⁴⁷ A. Foland,²¹ S. Forrester,⁷ G. W. Foster,¹⁶ M. Franklin,²¹ J. C. Freeman,²⁸ I. Furic,¹³ M. Gallinaro,⁵⁰ J. Galyardt,¹² J. E. Garcia,⁴⁶ M. Garcia Sciveres,²⁸ A. F. Garfinkel,⁴⁸ C. Gay,⁶⁰ H. Gerberich,²³ D. Gerdes,³⁴ S. Giagu,⁵¹ P. Giannetti,⁴⁶ A. Gibson,²⁸ K. Gibson,¹² C. Ginsburg,¹⁶ N. Giokaris,¹⁴ K. Giolo,⁴⁸ M. Giordani,⁵⁴ P. Giromini,¹⁸ M. Giunta,⁴⁶ G. Giurgiu,¹² V. Glagolev,¹⁴ D. Glenzinski,¹⁶ M. Gold,³⁷ N. Goldschmidt,³⁴ J. Goldstein,⁴² G. Gomez,¹¹ G. Gomez-Ceballos,¹¹ M. Goncharov,⁵³ O. González,³¹ I. Gorelov,³⁷ A. T. Goshaw,¹⁵ Y. Gotra,⁴⁷ K. Goulianos,⁵⁰ A. Greselle,⁴³ M. Griffiths,²⁹ S. Grinstein,²¹ C. Grossi-Pilcher,¹³ R. C. Group,¹⁷ U. Grundler,²³ J. Guimaraes da Costa,²¹ Z. Gunay-Unalan,³⁵ C. Haber,²⁸ S. R. Hahn,¹⁶ K. Hahn,⁴⁵ E. Halkiadakis,⁵² A. Hamilton,³³ B.-Y. Han,⁴⁹ J. Y. Han,⁴⁹ R. Handler,⁵⁹ F. Happacher,¹⁸ K. Hara,⁵⁵ M. Hare,⁵⁶ S. Harper,⁴² R. F. Harr,⁵⁸ R. M. Harris,¹⁶ K. Hatakeyama,⁵⁰ J. Hauser,⁸ C. Hays,¹⁵ A. Heijboer,⁴⁵ B. Heinemann,²⁹ J. Heinrich,⁴⁵ M. Herndon,⁵⁹ D. Hidas,¹⁵ C. S. Hill,¹⁰ D. Hirschbuehl,²⁵ A. Hocker,¹⁶ A. Holloway,²¹ S. Hou,¹ M. Houlden,²⁹ S.-C. Hsu,⁹ B. T. Huffman,⁴² R. E. Hughes,³⁹ J. Huston,³⁵ J. Incandela,¹⁰ G. Introzzi,⁴⁶ M. Iori,⁵¹ Y. Ishizawa,⁵⁵ A. Ivanov,⁷ B. Iyutin,³² E. James,¹⁶ D. Jang,⁵² B. Jayatilaka,³⁴ D. Jeans,⁵¹ H. Jensen,¹⁶ E. J. Jeon,²⁷ S. Jindariani,¹⁷ M. Jones,⁴⁸ K. K. Joo,²⁷ S. Y. Jun,¹² T. R. Junk,²³ T. Kamon,⁵³ J. Kang,³⁴ P. E. Karchin,⁵⁸ Y. Kato,⁴¹ Y. Kemp,²⁵ R. Kephart,¹⁶ U. Kerzel,²⁵ V. Khotilovich,⁵³ B. Kilminster,³⁹ D. H. Kim,²⁷ H. S. Kim,²⁷ J. E. Kim,²⁷ M. J. Kim,¹² S. B. Kim,²⁷ S. H. Kim,⁵⁵ Y. K. Kim,¹³ L. Kirsch,⁶ S. Klimentko,¹⁷ M. Klute,³² B. Knuteson,³² B. R. Ko,¹⁵ H. Kobayashi,⁵⁵ K. Kondo,⁵⁷ D. J. Kong,²⁷ J. Konigsberg,¹⁷ A. Korytov,¹⁷ A. V. Kotwal,¹⁵ A. Kovalev,⁴⁵ A. Kraan,⁴⁵ J. Kraus,²³ I. Kravchenko,³² M. Kreps,²⁵ J. Kroll,⁴⁵ N. Krummack,⁴ M. Kruse,¹⁵ V. Krutelyov,⁵³ S. E. Kuhlmann,² Y. Kusakabe,⁵⁷ S. Kwang,¹³ A. T. Laasanen,⁴⁸ S. Lai,³³ S. Lami,⁴⁶ S. Lammel,¹⁶ M. Lancaster,³⁰ R. L. Lander,⁷ K. Lannon,³⁹ A. Lath,⁵² G. Latino,⁴⁶ I. Lazzizzera,⁴³ T. LeCompte,² J. Lee,⁴⁹ J. Lee,²⁷ Y. J. Lee,²⁷ S. W. Lee,⁵³ R. Lefèvre,³ N. Leonardo,³² S. Leone,⁴⁶ S. Levy,¹³ J. D. Lewis,¹⁶ C. Lin,⁶⁰ C. S. Lin,¹⁶ M. Lindgren,¹⁶ E. Lipeles,⁹ T. M. Liss,²³ A. Lister,¹⁹ D. O. Litvintsev,¹⁶ T. Liu,¹⁶ N. S. Lockyer,⁴⁵ A. Loginov,³⁶ M. Loretta,⁴³ P. Loverre,⁵¹ R.-S. Lu,¹ D. Lucchesi,⁴³ P. Lujan,²⁸ P. Lukens,¹⁶ G. Lungu,¹⁷ L. Lyons,⁴² J. Lys,²⁸ R. Lysak,¹ E. Lytken,⁴⁸ P. Mack,²⁵ D. MacQueen,³³ R. Madrak,¹⁶ K. Maeshima,¹⁶ T. Maki,²² P. Maksimovic,²⁴ S. Malde,⁴² G. Manca,²⁹ F. Margaroli,⁵ R. Marginean,¹⁶ C. Marino,²³ A. Martin,⁶⁰ V. Martin,³⁸ M. Martínez,³ T. Maruyama,⁵⁵ H. Matsunaga,⁵⁵ M. E. Mattson,⁵⁸ R. Mazini,³³ P. Mazzanti,⁵ K. S. McFarland,⁴⁹ P. McIntyre,⁵³ R. McNulty,²⁹ A. Mehta,²⁹ S. Menzemer,¹¹ A. Menzione,⁴⁶ P. Merkel,⁴⁸ C. Mesropian,⁵⁰ A. Messina,⁵¹ M. von der Mey,⁸ T. Miao,¹⁶ N. Miladinovic,⁶ J. Miles,³² R. Miller,³⁵ J. S. Miller,³⁴ C. Mills,¹⁰ M. Milnik,²⁵ R. Miquel,²⁸ A. Mitra,¹ G. Mitselmakher,¹⁷ A. Miyamoto,²⁶ N. Moggi,⁵ B. Mohr,⁸ R. Moore,¹⁶ M. Morello,⁴⁶ P. Movilla Fernandez,²⁸ J. Mülmenstädt,²⁸ A. Mukherjee,¹⁶ Th. Muller,²⁵ R. Mumford,²⁴ P. Murat,¹⁶ J. Nachtman,¹⁶ J. Naganoma,⁵⁷ S. Nahm,³² I. Nakano,⁴⁰ A. Napier,⁵⁶ D. Naumov,³⁷ V. Necula,¹⁷ C. Neu,⁴⁵ M. S. Neubauer,⁹ J. Nielsen,²⁸ T. Nigmanov,⁴⁷ L. Nodulman,² O. Norniella,³ E. Nurse,³⁰ T. Ogawa,⁵⁷ S. H. Oh,¹⁵

Y. D. Oh,²⁷ T. Okusawa,⁴¹ R. Oldeman,²⁹ R. Orava,²² K. Osterberg,²² C. Pagliarone,⁴⁶ E. Palencia,¹¹ R. Paoletti,⁴⁶ V. Papadimitriou,¹⁶ A. A. Paramonov,¹³ B. Parks,³⁹ S. Pashapour,³³ J. Patrick,¹⁶ G. Paulette,⁵⁴ M. Paulini,¹² C. Paus,³² D. E. Pellett,⁷ A. Penzo,⁵⁴ T. J. Phillips,¹⁵ G. Piacentino,⁴⁶ J. Piedra,⁴⁴ L. Pinera,¹⁷ K. Pitts,²³ C. Plager,⁸ L. Pondrom,⁵⁹ X. Portell,³ O. Poukhov,¹⁴ N. Pounder,⁴² F. Prakoshyn,¹⁴ A. Pronko,¹⁶ J. Proudfoot,² F. Ptahos,¹⁸ G. Punzi,⁴⁶ J. Pursley,²⁴ J. Rademacker,⁴² A. Rahaman,⁴⁷ A. Rakitin,³² S. Rappoccio,²¹ F. Ratnikov,⁵² B. Reisert,¹⁶ V. Rekovic,³⁷ N. van Remortel,²² P. Renton,⁴² M. Rescigno,⁵¹ S. Richter,²⁵ F. Rimondi,⁵ L. Ristori,⁴⁶ W. J. Robertson,¹⁵ A. Robson,²⁰ T. Rodrigo,¹¹ E. Rogers,²³ S. Rolli,⁵⁶ R. Roser,¹⁶ M. Rossi,⁵⁴ R. Rossin,¹⁷ C. Rott,⁴⁸ A. Ruiz,¹¹ J. Russ,¹² V. Rusu,¹³ H. Saarikko,²² S. Sabik,³³ A. Safonov,⁵³ W. K. Sakumoto,⁴⁹ G. Salamanna,⁵¹ O. Saltó,³ D. Saltzberg,⁸ C. Sanchez,³ L. Santi,⁵⁴ S. Sarkar,⁵¹ L. Sartori,⁴⁶ K. Sato,⁵⁵ P. Savard,³³ A. Savoy-Navarro,⁴⁴ T. Scheidle,²⁵ P. Schlabach,¹⁶ E. E. Schmidt,¹⁶ M. P. Schmidt,⁶⁰ M. Schmitt,³⁸ T. Schwarz,³⁴ L. Scodellaro,¹¹ A. L. Scott,¹⁰ A. Scribano,⁴⁶ F. Scuri,⁴⁶ A. Sedov,⁴⁸ S. Seidel,³⁷ Y. Seiya,⁴¹ A. Semenov,¹⁴ L. Sexton-Kennedy,¹⁶ I. Sfiligoi,¹⁸ M. D. Shapiro,²⁸ T. Shears,²⁹ P. F. Shepard,⁴⁷ D. Sherman,²¹ M. Shimojima,⁵⁵ M. Shochet,¹³ Y. Shon,⁵⁹ I. Shreyber,³⁶ A. Sidoti,⁴⁴ P. Sinervo,³³ A. Sisakyan,¹⁴ J. Sjolin,⁴² A. Skiba,²⁵ A. J. Slaughter,¹⁶ K. Sliwa,⁵⁶ J. R. Smith,⁷ F. D. Snider,¹⁶ R. Snihur,³³ M. Soderberg,³⁴ A. Soha,⁷ S. Somalwar,⁵² V. Sorin,³⁵ J. Spalding,¹⁶ M. Spezziga,¹⁶ F. Spinella,⁴⁶ T. Spreitzer,³³ P. Squillacioti,⁴⁶ M. Stanitzki,⁶⁰ A. Staveris-Polykalas,⁴⁶ R. St. ****Denis,²⁰ B. Stelzer,⁸ O. Stelzer-Chilton,⁴² D. Stentz,³⁸ J. Strologas,³⁷ D. Stuart,¹⁰ J. S. Suh,²⁷ A. Sukhanov,¹⁷ K. Sumorok,³² H. Sun,⁵⁶ T. Suzuki,⁵⁵ A. Taffard,²³ R. Takashima,⁴⁰ Y. Takeuchi,⁵⁵ K. Takikawa,⁵⁵ M. Tanaka,² R. Tanaka,⁴⁰ N. Tanimoto,⁴⁰ M. Tecchio,³⁴ P. K. Teng,¹ K. Terashi,⁵⁰ S. Tether,³² J. Thom,¹⁶ A. S. Thompson,²⁰ E. Thomson,⁴⁵ P. Tipton,⁴⁹ V. Tiwari,¹² S. Tkaczyk,¹⁶ D. Toback,⁵³ S. Tokar,¹⁴ K. Tollefson,³⁵ T. Tomura,⁵⁵ D. Tonelli,⁴⁶ M. Tönnesmann,³⁵ S. Torre,¹⁸ D. Torretta,¹⁶ S. Tourneur,⁴⁴ W. Trischuk,³³ R. Tsuchiya,⁵⁷ S. Tsuno,⁴⁰ N. Turini,⁴⁶ F. Ukegawa,⁵⁵ T. Unverhau,²⁰ S. Uozumi,⁵⁵ D. Usynin,⁴⁵ A. Vaiciulis,⁴⁹ S. Vallecorsa,¹⁹ A. Varganov,³⁴ E. Vataga,³⁷ G. Velev,¹⁶ G. Veramendi,²³ V. Veszpremi,⁴⁸ R. Vidal,¹⁶ I. Vila,¹¹ R. Vilar,¹¹ T. Vine,³⁰ I. Vollrath,³³ I. Volobouev,²⁸ G. Volpi,⁴⁶ F. Würthwein,⁹ P. Wagner,⁵³ R. G. Wagner,² R. L. Wagner,¹⁶ W. Wagner,²⁵ R. Wallny,⁸ T. Walter,²⁵ Z. Wan,⁵² S. M. Wang,¹ A. Warburton,³³ S. Waschke,²⁰ D. Waters,³⁰ W. C. Wester III,¹⁶ B. Whitehouse,⁵⁶ D. Whiteson,⁴⁵ A. B. Wicklund,² E. Wicklund,¹⁶ G. Williams,³³ H. H. Williams,⁴⁵ P. Wilson,¹⁶ B. L. Winer,³⁹ P. Wittich,¹⁶ S. Wolbers,¹⁶ C. Wolfe,¹³ T. Wright,³⁴ X. Wu,¹⁹ S. M. Wynne,²⁹ A. Yagil,¹⁶ K. Yamamoto,⁴¹ J. Yamaoka,⁵² T. Yamashita,⁴⁰ C. Yang,⁶⁰ U. K. Yang,¹³ Y. C. Yang,²⁷ W. M. Yao,²⁸ G. P. Yeh,¹⁶ J. Yoh,¹⁶ K. Yorita,¹³ T. Yoshida,⁴¹ G. B. Yu,⁴⁹ I. Yu,²⁷ S. S. Yu,¹⁶ J. C. Yun,¹⁶ L. Zanello,⁵¹ A. Zanetti,⁵⁴ I. Zaw,²¹ F. Zetti,⁴⁶ X. Zhang,²³ J. Zhou,⁵² and S. Zucchelli⁵

(CDF Collaboration)

¹*Institute of Physics, Academia Sinica, Taipei, Taiwan 11529, Republic of China*²*Argonne National Laboratory, Argonne, Illinois 60439, USA*³*Institut de Fisica d'Altes Energies, Universitat Autònoma de Barcelona, E-08193, Bellaterra (Barcelona), Spain*⁴*Baylor University, Waco, Texas 76798, USA*⁵*Istituto Nazionale di Fisica Nucleare, University of Bologna, I-40127 Bologna, Italy*⁶*Brandeis University, Waltham, Massachusetts 02254, USA*⁷*University of California-Davis, Davis, California 95616, USA*⁸*University of California-Los Angeles, Los Angeles, California 90024, USA*⁹*University of California-San Diego, La Jolla, California 92093, USA*¹⁰*University of California-Santa Barbara, Santa Barbara, California 93106, USA*¹¹*Instituto de Fisica de Cantabria, CSIC-University of Cantabria, 39005 Santander, Spain*¹²*Carnegie Mellon University, Pittsburgh, Pennsylvania 15213, USA*¹³*Enrico Fermi Institute, University of Chicago, Chicago, Illinois 60637, USA*¹⁴*Joint Institute for Nuclear Research, RU-141980 Dubna, Russia*¹⁵*Duke University, Durham, North Carolina 27708, USA*¹⁶*Fermi National Accelerator Laboratory, Batavia, Illinois 60510, USA*¹⁷*University of Florida, Gainesville, Florida 32611, USA*¹⁸*Laboratori Nazionali di Frascati, Istituto Nazionale di Fisica Nucleare, I-00044 Frascati, Italy*¹⁹*University of Geneva, CH-1211 Geneva 4, Switzerland*²⁰*Glasgow University, Glasgow G12 8QQ, United Kingdom*²¹*Harvard University, Cambridge, Massachusetts 02138, USA*²²*Division of High Energy Physics, Department of Physics, University of Helsinki and Helsinki Institute of Physics, FIN-00014, Helsinki, Finland*²³*University of Illinois, Urbana, Illinois 61801, USA*

²⁴*The Johns Hopkins University, Baltimore, Maryland 21218, USA*²⁵*Institut für Experimentelle Kernphysik, Universität Karlsruhe, 76128 Karlsruhe, Germany*²⁶*High Energy Accelerator Research Organization (KEK), Tsukuba, Ibaraki 305, Japan*²⁷*Center for High Energy Physics: Kyungpook National University, Taegu 702-701, Korea; Seoul National University, Seoul 151-742, Korea; and SungKyunKwan University, Suwon 440-746, Korea*²⁸*Ernest Orlando Lawrence Berkeley National Laboratory, Berkeley, California 94720, USA*²⁹*University of Liverpool, Liverpool L69 7ZE, United Kingdom*³⁰*University College London, London WC1E 6BT, United Kingdom*³¹*Centro de Investigaciones Energeticas Medioambientales y Tecnologicas, E-28040 Madrid, Spain*³²*Massachusetts Institute of Technology, Cambridge, Massachusetts 02139, USA*³³*Institute of Particle Physics: McGill University, Montréal, Canada H3A 2T8;**and University of Toronto, Toronto, Canada M5S 1A7*³⁴*University of Michigan, Ann Arbor, Michigan 48109, USA*³⁵*Michigan State University, East Lansing, Michigan 48824, USA*³⁶*Institution for Theoretical and Experimental Physics, ITEP, Moscow 117259, Russia*³⁷*University of New Mexico, Albuquerque, New Mexico 87131, USA*³⁸*Northwestern University, Evanston, Illinois 60208, USA*³⁹*The Ohio State University, Columbus, Ohio 43210, USA*⁴⁰*Okayama University, Okayama 700-8530, Japan*⁴¹*Osaka City University, Osaka 588, Japan*⁴²*University of Oxford, Oxford OX1 3RH, United Kingdom*⁴³*University of Padova, Istituto Nazionale di Fisica Nucleare, Sezione di Padova-Trento, I-35131 Padova, Italy*⁴⁴*LPNHE, Université Pierre et Marie Curie/IN2P3-CNRS, UMR7585, Paris, F-75252 France*⁴⁵*University of Pennsylvania, Philadelphia, Pennsylvania 19104, USA*⁴⁶*Istituto Nazionale di Fisica Nucleare Pisa, Universities of Pisa, Siena and Scuola Normale Superiore, I-56127 Pisa, Italy*⁴⁷*University of Pittsburgh, Pittsburgh, Pennsylvania 15260, USA*⁴⁸*Purdue University, West Lafayette, Indiana 47907, USA*⁴⁹*University of Rochester, Rochester, New York 14627, USA*⁵⁰*The Rockefeller University, New York, New York 10021, USA*⁵¹*Istituto Nazionale di Fisica Nucleare, Sezione di Roma I, University of Rome "La Sapienza," I-00185 Roma, Italy*⁵²*Rutgers University, Piscataway, New Jersey 08855, USA*⁵³*Texas A&M University, College Station, Texas 77843, USA*⁵⁴*Istituto Nazionale di Fisica Nucleare, University of Trieste/Udine, Italy*⁵⁵*University of Tsukuba, Tsukuba, Ibaraki 305, Japan*⁵⁶*Tufts University, Medford, Massachusetts 02155, USA*⁵⁷*Waseda University, Tokyo 169, Japan*⁵⁸*Wayne State University, Detroit, Michigan 48201, USA*⁵⁹*University of Wisconsin, Madison, Wisconsin 53706, USA*⁶⁰*Yale University, New Haven, Connecticut 06520, USA*

(Received 9 March 2006; published 7 July 2006)

We present a measurement of the B_c^+ meson lifetime in the decay mode $B_c^+ \rightarrow J/\psi e^+ \nu_e$ using the Collider Detector at Fermilab II detector at the Fermilab Tevatron Collider. From a sample of about 360 pb^{-1} of $p\bar{p}$ collisions at $\sqrt{s} = 1.96 \text{ TeV}$, we reconstruct $J/\psi e^+$ pairs with invariant mass in the kinematically allowed range $4 < M_{J/\psi e} < 6 \text{ GeV}/c^2$. A fit to the decay-length distribution of 238 signal events yields a measured B_c^+ meson lifetime of $0.463^{+0.073}_{-0.065} (\text{stat}) \pm 0.036 (\text{syst}) \text{ ps}$.

DOI: 10.1103/PhysRevLett.97.012002

PACS numbers: 14.40.Nd, 13.20.He

The B_c^+ meson is the only known meson consisting of two heavy quarks of different flavor: a charm quark and a bottom antiquark. It provides a unique test of heavy-quark dynamics, since the bound state can be treated using the same nonrelativistic expansion that successfully describes both $c\bar{c}$ and $b\bar{b}$ families. However, unlike $c\bar{c}$ and $b\bar{b}$ states, the B_c^+ meson decays only via weak interactions, thus having a measurable lifetime. The lifetime of the B_c^+ meson is expected to be about 2–3 times smaller than the B^+ meson lifetime if one assumes three major decay subprocesses [1,2]: \bar{b} quark decay with the c quark as a

spectator, c quark decay with the \bar{b} quark as a spectator, and $\bar{b}c$ annihilation decays. In the B^+ meson case, the dominant decay subprocess is the \bar{b} quark decay with the u quark as a spectator. An early measurement from CDF [3] found a B_c^+ lifetime consistent with predictions. More precise measurements will determine the relative importance of the three decay subprocesses and provide insight into the strong dynamics of heavy quarks. Here we report a new B_c^+ meson lifetime measurement using the decay mode $B_c^+ \rightarrow J/\psi e^+ \nu_e$, where charge-conjugate modes are implied, from a sample of 360 pb^{-1} collected during

2002–2004 with the CDF II detector [4] at the Fermilab Tevatron Collider at a center of mass energy of 1.96 TeV. The new measurement is about 2.5 times more precise than the previous one.

The $B_c^+ \rightarrow J/\psi e^+ \nu_e$ reconstruction starts with $J/\psi \rightarrow \mu^+ \mu^-$ candidates selected based upon a two-muon topology by the CDF trigger system [5]. The J/ψ candidates are further purified during offline reconstruction by vertex constraining the $\mu^+ \mu^-$ pairs and by selecting the pairs with momentum transverse to the beam line $p_{T_{J/\psi}} > 3$ GeV/c. Then each J/ψ candidate with a reconstructed mass within 50 MeV/c² of its nominal value is combined with an electron to form a B_c^+ candidate.

Electron identification uses both specific ionization (dE/dx) information from the central outer tracker (COT) and calorimeter shower information from the central electromagnetic calorimeter (CEM). The logarithm of the ratio of the measured dE/dx value from a charged particle to that expected for an electron, $Z_e = \ln(dE/dx) - \ln(dE/dx)_{\text{predict}}$, is compared to its standard deviation σ_{Z_e} . The expected dE/dx and σ_{Z_e} are functions of the particle charge, momentum, and the multiplicity of associated COT hits. Electron candidates are required to have $Z_e/\sigma_{Z_e} > -1.3$ to reject hadrons ($\pi/K/p$) while remaining efficient for true electrons. Samples of electrons, pions, kaons, and protons selected from collision data are used to determine the dE/dx identification efficiencies listed in Table I. These control samples come from photon conversions $\gamma \rightarrow e^+ e^-$ and from hadron decays $K^0 \rightarrow \pi^+ \pi^-$, $D^0 \rightarrow K^- \pi^+$, and $\Lambda^0 \rightarrow p \pi^-$. The hadrons surviving the Z_e/σ_{Z_e} selection are mainly pions, which are rejected using calorimeter shower shape information.

The calorimeter shower shape of a charged particle with $p_T > 2$ GeV/c is obtained by extrapolating its track reconstructed in the COT into the calorimeter to match shower clusters there [3]. The probabilities for a particle to have a shower shape consistent with being an electron or a hadron are calculated using the distributions of shower energy and shower cluster profiles for the electron and hadron samples described above. We first define the proba-

bility for a charged particle to be an electron based on shower shape by the ratio between its probability to be an electron and the sum of its probabilities to be an electron or a hadron. We then obtain a cumulative probability distribution of the ratio using the electron sample and impose a selection on electron candidates at a 70% probability value. To calculate the average probability for hadrons to pass this requirement, as listed in Table I, the control samples of $\pi/K/p$ particles are mixed using fractions predicted by a PYTHIA Monte Carlo (MC) simulation of $B \rightarrow J/\psi X$ events [6]. In addition, electrons found to originate from photon conversion $\gamma \rightarrow e^+ e^-$ are removed from consideration as $J/\psi e^+$ candidates [3]. Overall, the electron identification using combined dE/dx and calorimeter information has an efficiency of 60% for true electrons, while hadrons have a probability to pass the selection lower than 0.15%.

A B_c^+ candidate is a $J/\psi e^+$ pair with transverse momentum $p_{T_{J/\psi e}} > 5$ GeV/c and invariant mass $4 < M_{J/\psi e} < 6$ GeV/c². The upper bound on $M_{J/\psi e}$ is simply the kinematic limit from the mass of B_c^+ meson [7]. The lower bound is set higher than the kinematic limit of $M_{J/\psi}$ to reduce the background from B_c^+ semileptonic decays other than the exclusive decay $B_c^+ \rightarrow J/\psi e^+ \nu_e$ to a few percent [1,3]. The opening angle between the J/ψ and electron momenta in the transverse plane must be within 90° to reduce generic $b\bar{b}$ background that produces a J/ψ and an electron from different b hadrons. Finally, the tracks of the three daughter particles μ^+ , μ^- , and e^+ are fit to a common vertex, and the B_c^+ decay length in the transverse plane L_{xy} is calculated as the projection of the displacement of the B_c^+ vertex from the primary vertex onto the momentum of the $J/\psi e^+$ system. The primary vertex position is obtained from run-by-run averages using samples of prompt tracks.

Before making a lifetime measurement, we first establish the B_c^+ signal in the $J/\psi e^+$ pairs. The background pairs from prompt decays are removed by imposing a selection of $L_{xy}/\sigma_{L_{xy}} > 3$. The $M_{J/\psi e}$ distribution of $J/\psi e^+$ pairs with $L_{xy}/\sigma_{L_{xy}} > 3$ is shown in Fig. 1.

TABLE I. Electron identification efficiencies (percent) as functions of particle p_T (GeV/c) using dE/dx and a calorimeter (Cal) for electron and hadrons. The dE/dx results are averages of positively and negatively charged particles. The calorimeter results for hadrons (h) are the weighted averages of π , K , and p . The conversion-finding efficiency ϵ_{conv} is also listed.

p_T	2–3	3–4	4–5	5–6	>6
$dE/dx: e$	91.3 ± 0.1	91.4 ± 0.2	90.7 ± 0.2	90.5 ± 0.3	89.5 ± 0.2
$dE/dx: \pi$	16.4 ± 0.1	23.8 ± 0.1	32.0 ± 0.1	39.0 ± 0.2	49.4 ± 0.2
$dE/dx: K$	2.09 ± 0.09	2.35 ± 0.07	3.29 ± 0.09	4.4 ± 0.1	9.5 ± 0.2
$dE/dx: p$	3.38 ± 0.03	2.14 ± 0.04	2.54 ± 0.07	3.0 ± 0.1	4.9 ± 0.2
Cal: e^+	68.5 ± 0.3	68.8 ± 0.5	68.9 ± 0.8	68.9 ± 1.1	67.6 ± 1.0
Cal: e^-	67.9 ± 0.4	69.5 ± 0.5	69.6 ± 0.7	68.1 ± 1.2	68.5 ± 0.9
Cal: h^+	0.77 ± 0.04	0.37 ± 0.04	0.37 ± 0.03	0.29 ± 0.04	0.13 ± 0.04
Cal: h^-	0.64 ± 0.04	0.37 ± 0.02	0.27 ± 0.03	0.25 ± 0.04	0.21 ± 0.04
ϵ_{conv}	49.8 ± 1.4	55.0 ± 2.2	56.5 ± 3.3	61.5 ± 4.5	69.2 ± 3.4

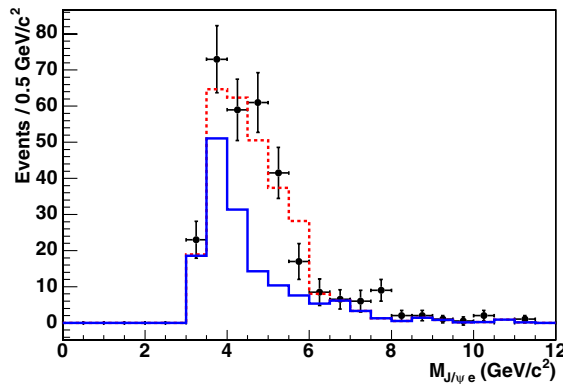


FIG. 1 (color online). $M_{J/\psi e}$ distribution of $J/\psi e^+$ pairs (dots with error bars) with $L_{xy}/\sigma_{L_{xy}} > 3$ together with the expected shape (dashed line) from a sum of a MC signal and the estimated background (solid lines) which is mostly from b -hadron decays. The false J/ψ is already removed in the distribution.

Within the $4 < M_{J/\psi e} < 6$ GeV/ c^2 window, 203 candidates are found with a total of background 88 ± 14 as listed in Table II. The background is classified into four groups: (i) background with a false J/ψ , background with a correctly identified J/ψ but a wrong electron candidate which can be either (ii) a misidentified hadron (false electron) or (iii) an electron from photon to e^+e^- conversion, and (iv) background from decays of other B hadrons ($b\bar{b}$). The number of false J/ψ backgrounds is estimated using $\mu^+\mu^-$ pairs with an invariant mass outside the 50 MeV/ c^2 window. To estimate the false electron background, we use a sample of J/ψ -track pairs passing the same selection as the $J/\psi e^+$ pairs, including the dE/dx requirement and the requirement to point to the CEM fiducial region, but without any selection based on calorimeter information. The size of the contribution is estimated from a weighted counting of the J/ψ -track pairs with the weights taken as the averaged probabilities in Table I for hadrons to pass the electron selection using the calorimeter. We derive the residual conversion electron contribution from the rate of identified photon conversions together with the conversion-finding efficiency listed in Table I. The conversion-finding efficiency, defined as the

TABLE II. Numbers of $J/\psi e^+$ pairs and estimated backgrounds. The error listed is the sum of statistical and systematic errors.

	All L_{xy}	$L_{xy}/\sigma_{L_{xy}} > 3$
False J/ψ	164.0 ± 9.1	24.5 ± 3.5
False electron	110.2 ± 19.0	15.4 ± 2.5
Conversion electron	67.4 ± 34.8	14.5 ± 7.8
$b\bar{b}$	63.0 ± 18.5	33.6 ± 11.4
Prompt decay	141.7 ± 32.0	...
Total background	545 ± 55	88 ± 14
Observed $J/\psi e^+$ pairs	783	203

fraction of the identified electrons with their conversion partners in the kinematic acceptance of the CDF detector, is estimated from a MC simulation. Finally, the contribution from decays resulting from $b\bar{b}$ production is estimated using a PYTHIA MC sample with relative rates of flavor creation, flavor excitation, and gluon splitting tuned to the Tevatron data [6,8]. The number of B_c^+ signal events is found to be $115 \pm 16(\text{stat}) \pm 14(\text{syst})$. For comparison, there are 2872 ± 59 $B^+ \rightarrow J/\psi K^+$ events in the data sample corresponding to the same integrated luminosity. The selection of B^+ is the same as for B_c^+ except for electron identification on the K^+ . We find the production rate of B_c^+ relative to that of B^+ , $[\sigma(B_c^+)B(B_c^+ \rightarrow J/\psi X e^+ \nu_e)]/[\sigma(B^+)B(B^+ \rightarrow J/\psi K^+)]$, in the kinematic range $p_T > 4$ GeV/ c and rapidity $|y| < 1$ [7] to be $0.282 \pm 0.038(\text{stat}) \pm 0.035(\text{syst}) \pm 0.065(\text{acceptance})$. The first error is statistical, the second covers the systematic uncertainty of B_c^+ signal excess counting, and the third pertains to the estimated detector acceptance ratio correction $A_{B^+}/A_{B_c^+} = 4.42 \pm 1.02$ from MC simulation where the B_c^+ p_T spectrum, its lifetime values, and decay modes are the major sources of uncertainty. This new production ratio result agrees with the earlier CDF measurement [3].

Having established a clear B_c^+ signal in $J/\psi e^+$ combinations, we measure the B_c^+ meson lifetime in a larger sample of 783 events, selected with the same criteria as above, but without the L_{xy} selection. We estimate the net signal excess in this sample to be 238. The background sources and their contributions are listed in Table II. Contributions from false electrons, conversion electrons, $b\bar{b}$, and false J/ψ are estimated as described earlier. The number of additional prompt-decay events is extracted directly from the lifetime fit.

The Lorentz-invariant proper decay time of a B_c^+ event is its decay length L_{xy} with a Lorentz boost $\beta\gamma = p_{T_{B_c}}/M_{B_c}$ in the transverse plane, where M_{B_c} is the mass of B_c^+ meson and $p_{T_{B_c}}$ its transverse momentum. The B_c^+ mass is assumed to have a value of 6.271 GeV/ c^2 [2]. Because of the missing neutrino, we cannot directly calculate the boost factor from the lab system to the B_c^+ rest frame. We can, however, calculate the B_c^+ lifetime in the center of mass frame of the $J/\psi e^+$ pair, $ct' = L_{xy}M_{J/\psi e}/p_{T_{J/\psi e}}$, which provides the best estimator of the B_c^+ proper decay time in the absence of the neutrino momentum. The true proper B_c^+ decay time is given by $ct = L_{xy}p_{T_{B_c}}/M_{B_c} = K \cdot ct'$, where K is the residual correction factor depending on the momenta of the missing neutrino. In MC simulations, K can be calculated $K \equiv (p_{T_{J/\psi e}}/p_{T_{B_c}})(M_{B_c}/M_{J/\psi e})\cos\alpha$, where α is the angle between the vectors of $p_{T_{J/\psi e}}$ and $p_{T_{B_c}}$. The K distributions, as shown in Fig. 2, always include $K = 1$ and decrease in width as $M_{J/\psi e}$ gets closer to the value of B_c^+ mass when the neutrino's momentum is minimal.

An unbinned maximum-likelihood fit [3,4] is used to extract the B_c^+ meson lifetime. In the fit, t' and its event-by-

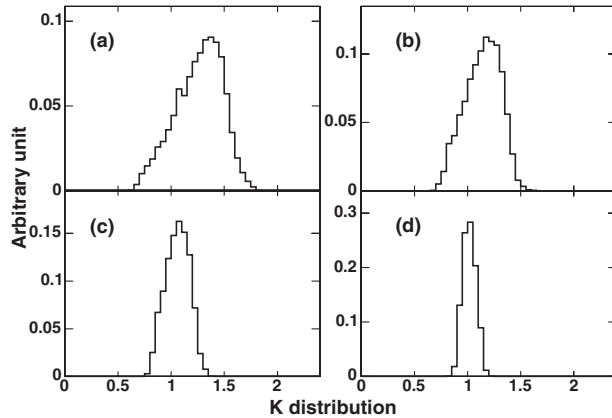


FIG. 2. Distribution of K for $M_{J/\psi e}$ within (a) 4–4.5, (b) 4.5–5.0, (c) 5.0–5.5, and (d) 5.5–6.0 GeV/c^2 .

event error $\sigma_{t'} = \sigma_{L_{xy}} M_{J/\psi e} / (c p_{T_{J/\psi e}})$ are the input variables. The likelihood function has the form [9] $\mathcal{F}(t', \sigma_{t'}) = (1 - \sum_1^5 f_{b_i}) \mathcal{F}_s(t', \sigma_{t'}) \mathcal{P}_s(\sigma_{t'}) + \sum_1^5 f_{b_i} \mathcal{F}_{b_i}(t', \sigma_{t'}) \mathcal{P}_{b_i}(\sigma_{t'})$, where $\mathcal{F}_s(t', \sigma_{t'})$ is the lifetime probability density function (PDF) for a pure B_c^+ signal, f_{b_i} and $\mathcal{F}_{b_i}(t', \sigma_{t'})$ are fractions of the five background contributions and their lifetime PDFs, and $\mathcal{P}_s(\sigma_{t'})$ and $\mathcal{P}_{b_i}(\sigma_{t'})$ are the PDFs of the $\sigma_{t'}$ for signal and backgrounds. The lifetime PDF for the B_c^+ signal is an exponential lifetime distribution convoluted with the K distribution and a Gaussian resolution function. The prompt background lifetime PDF is assumed to have zero lifetime with a Gaussian resolution function. The PDFs for other backgrounds are described by a sum of a Gaussian distribution centered at zero and two pairs of positive and negative exponential lifetime functions with no K correction applied. The initial parameters for these background PDFs are obtained from fits to the background samples as shown in Fig. 3. The obtained results are used to constrain the corresponding parameters in the final lifetime fit. The constraints are imposed by multiplying the likelihood function with Gaussian functions of the appropriate mean and width. Similarly, the background fractions f_{b_i} are also constrained in the B_c^+ meson lifetime fit to the estimated values in Table II.

In Fig. 4, the ct' distribution from the 783 B_c^+ candidates is shown with the fit result superimposed. We find $c\tau_{B_c} = 139^{+22}_{-20} \mu\text{m}$. The sources of systematic uncertainty on the lifetime fit are now considered, and their magnitudes are estimated. The effect of the K distribution uncertainty on the B_c^+ lifetime fit is estimated using alternative K distributions obtained from MC simulations with different p_T spectrum, mass, and lifetime values, and B_c^+ meson decay modes. The p_T spectrum is changed from that derived using a theoretical calculation [10] to that of the inclusive decay $B \rightarrow J/\psi X$ [4]. The mass and lifetime in the MC calculation are varied in the ranges $M_{B_c} = 6.2$ – $6.4 \text{ GeV}/c^2$ and $\tau_{B_c} = 0.4$ – 0.7 ps [1,2]. The B_c^+ decay considered in the MC calculation is varied from the exclusive $B_c^+ \rightarrow$

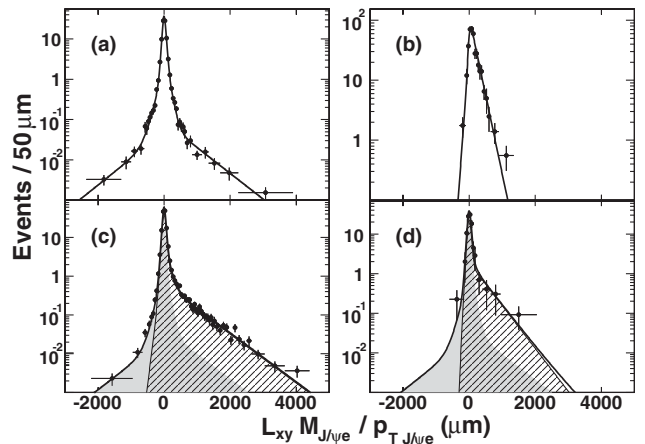


FIG. 3. ct' PDF obtained from fits to background samples (points with error bars) for (a) false J/ψ (solid lines), (b) $b\bar{b}$ (solid lines), (c) false electron (hatched area), and (d) conversion electron (hatched area). In (c) and (d), the solid lines are the sum of false J/ψ (shaded area) and a false or conversion electron. The false J/ψ fraction and lifetime shape in (c) and (d) are constrained to that obtained from sideband events.

$J/\psi e^+ \nu_e$ alone to that of an inclusive decay table predicted in Ref. [1]. We found the change on the B_c^+ lifetime fit as $\Delta c\tau_{B_c} = \pm 2.8 \mu\text{m}$. The uncertainty related to background lifetime shapes is estimated from investigating the p_T dependence of the electron identification and the conversion-finding efficiencies, from using false J/ψ events from different samples with or without an electron nearby, and from changing fractions of $b\bar{b}$ events originating from the three main production mechanisms according to a study using CDF data [8]. The estimated effect is $\pm 9.2 \mu\text{m}$. The uncertainty related to the L_{xy} calculation and its error distribution is found to be $\pm 4.7 \mu\text{m}$ from the uncertainty in the silicon detector alignment, by using an alternative functional form describing the L_{xy} resolution that includes an additional Gaussian and symmetric exponential tails, and by using alternative decay-length er-

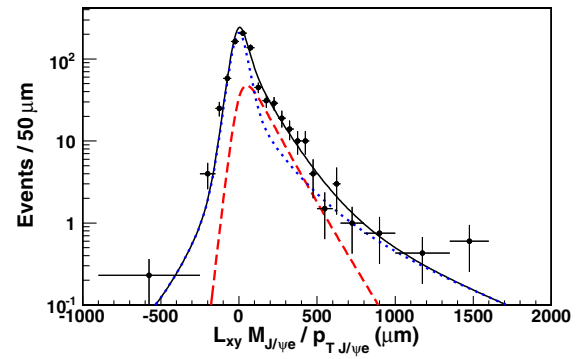


FIG. 4 (color online). ct' distribution from 783 B_c^+ candidates. The points with error bars are data points and the solid line is the fit result. The dashed line is the B_c^+ signal and the dotted line is the background.

ror distributions. The fitting procedure is also checked using MC ct' distributions similar to that of the B_c^+ candidates, and there is no bias found. Adding all the estimated systematic errors in quadrature, we find $c\tau_{B_c} = 139^{+22}_{-20}(\text{stat}) \pm 11(\text{syst}) \mu\text{m}$ or $\tau_{B_c} = 0.463^{+0.073}_{-0.065}(\text{stat}) \pm 0.036(\text{syst}) \text{ ps}$.

In conclusion, from an unbinned maximum-likelihood fit to the decay-length distribution of 238 signal events of $B_c^+ \rightarrow J/\psi e^+ \nu_e$, the B_c^+ meson lifetime is found to be $0.463^{+0.073}_{-0.065}(\text{stat}) \pm 0.036(\text{syst}) \text{ ps}$, which is about one-third of the B^+ meson lifetime of $1.671 \pm 0.018 \text{ ps}$ [7]. This agrees with theoretical models [1,2] in which all the three major decay subprocesses, the two spectator processes (\bar{b} -quark and c -quark) and the $\bar{b}c$ annihilation, play important roles in the B_c^+ decays.

We thank the Fermilab staff and the technical staffs of the participating institutions for their vital contributions. This work was supported by the U.S. Department of Energy and National Science Foundation; the Italian Istituto Nazionale di Fisica Nucleare; the Ministry of Education, Culture, Sports, Science and Technology of Japan; the Natural Sciences and Engineering Research Council of Canada; the National Science Council of the Republic of China; the Swiss National Science Foundation; the A.P. Sloan Foundation; the Bundesministerium für Bildung und Forschung, Germany; the Korean Science and Engineering Foundation and the Korean Research Foundation; the Particle Physics and

Astronomy Research Council and the Royal Society, United Kingdom; the Russian Foundation for Basic Research; the Comisión Interministerial de Ciencia y Tecnología, Spain; in part by the European Community's Human Potential Programme under Contract no. HPRN-CT-2002-00292; and the Academy of Finland.

-
- [1] V. V. Kiselev, hep-ph/0308214.
 - [2] S. Godfrey, Phys. Rev. D **70**, 054017 (2004).
 - [3] F. Abe *et al.* (CDF Collaboration), Phys. Rev. D **58**, 112004 (1998).
 - [4] D. Acosta *et al.* (CDF Collaboration), Phys. Rev. D **71**, 032001 (2005), and references therein.
 - [5] E. J. Thomson *et al.*, IEEE Trans. Nucl. Sci. **49**, 1063 (2002); A. Abulencia *et al.* (CDF Collaboration), Phys. Rev. Lett. **96**, 102002 (2006).
 - [6] T. Sjostrand *et al.*, Comput. Phys. Commun. **135**, 238 (2001); R. Field, Phys. Rev. D **65**, 094006 (2002).
 - [7] S. Eidelman *et al.*, Phys. Lett. B **592**, 1 (2004).
 - [8] D. Acosta *et al.* (CDF Collaboration), Phys. Rev. D **71**, 092001 (2005).
 - [9] G. Punzi, in *Proceedings of PHYSTAT2003: Statistical Problems in Particle Physics, Astrophysics and Cosmology, Menlo Park, CA, 2003*, edited by L. Lyons, R. Mount, and R. Reitmeyer, eConf C030908, WELT002 (2003).
 - [10] C. H. Chang *et al.*, Comput. Phys. Commun. **159**, 192 (2004).